

O₂ Chemistry of Dicopper Complexes with Alkyltriamine Ligands. Comparing Synergistic Effects on O₂ Binding

Anna Company,[†] Diana Lamata,[†] Albert Poater,[†] Miquel Solà,[†] Elena V. Rybak-Akimova,^{*,‡} Lawrence Que, Jr.,[§] Xavier Fontrodona,^{||} Teodor Parella,[⊥] Antoni Llobet,^ε and Miquel Costas^{*,†}

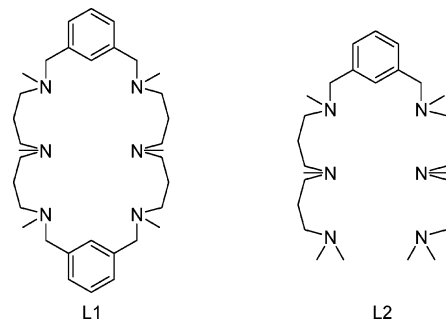
Departament de Química and Institut de Química Computacional, Universitat de Girona, Campus de Montilivi, E-17071 Girona, Catalonia, Spain, Department of Chemistry, Tufts University, Medford, Massachusetts 02155, Department of Chemistry, University of Minnesota, Minneapolis, Minnesota 55455, Serveis Científic-Tècnics, Universitat de Girona, Campus de Montilivi, E-17071 Girona, Spain, Servei de RMN, Universitat Autònoma de Barcelona, Bellaterra, E-08193, Spain, and Departament de Química, Universitat Autònoma de Barcelona, Bellaterra, E-08193 Barcelona, Spain

Received February 13, 2006

Two dicopper(I) complexes containing tertiary N-methylated hexaaza ligands which impose different steric constraints to the Cu ions have been synthesized, and their reactivity toward O₂ has been compared with a mononuclear related system, highlighting the importance of cooperative effects between the metal centers in O₂ activation.

A number of proteins involved in dioxygen transport and activation contain a dinuclear Cu active site.¹ The arguably best known are hemocyanin, catechol oxidase, and tyrosinase, which react with O₂ generating O₂-bound species which have been spectroscopically and structurally characterized.^{1,2} Traditionally, the mimicking of these dicopper centers was performed either using mononuclear complexes that self-assemble when reacting with O₂ or via dinucleating ligands designed with the purpose of favoring O₂ binding by spatial preorganization of the dimetallic site.³ Particularly remarkable are *m*-xylyl-linked dinuclear Cu(I) complexes which react with O₂ to form well-characterized (μ - η^2 : η^2 -peroxo)dicopper(II) species that in selected cases undergo intra-⁴ or

Scheme 1. Schematic Structure of Ligands L1 and L2



intermolecular⁵ regioselective hydroxylation of an aromatic ring, thus mimicking tyrosinase activity.

Here, we report the reactivity with O₂ of two related dinuclear copper(I) complexes supported by two hexaaza ligands (L1⁶ and L2, Scheme 1) based on a *m*-xylyl spacer and compare it with the one recently reported for the mononuclear analogue [Cu(MeAN)]B(C₆F₅)₄ (MeAN = *N,N,N',N',N''*-pentamethyldipropylentriamine).⁷ The three complexes contain ligands that bind copper atoms within very similar coordination environments and give rise to electronically and structurally comparable metal sites. However, they exhibit rather unexpected differences in their reaction with O₂ that may be understood on the basis of the relative ability of the ligand to promote a synergistic actuation of the two Cu ions along the O₂-binding process.

* To whom correspondence should be addressed. Fax: 34 972 41 81 50 (M.C.). E-mail: miquel.costas@udg.es (M.C.).

[†] Departament de Química and Institut de Química Computacional, Universitat de Girona.

[‡] Tufts University.

[§] University of Minnesota.

^{||} Serveis Científic-Tècnics, Universitat de Girona.

[⊥] Servei de RMN, Universitat Autònoma de Barcelona.

^ε Departament de Química, Universitat Autònoma de Barcelona.

- (1) (a) Solomon, E. I.; Sundaram, U. M.; Machonkin, T. E. *Chem. Rev.* **1996**, *96*, 2563. (b) Solomon, E. I.; Chen, P.; Metz, M.; Lee, S.-K.; Palmer, A. E. *Angew. Chem., Int. Ed.* **2001**, *40*, 4570.
- (2) (a) Magnus, K. A.; Ton-That, H.; Carpenter, J. E. *Chem. Rev.* **1994**, *94*, 727. (b) Matoba, Y.; Kumagai, T.; Yamamoto, A.; Yoshitsu H.; Sugiyama, M. *J. Biol. Chem.* **2006**, *281*, 8981.
- (3) (a) Mirica, L. M.; Ottenwaelder, X.; Stack, T. D. P. *Chem. Rev.* **2004**, *114*, 1013. (b) Lewis, E. A.; Tolman, W. B. *Chem. Rev.* **2004**, *114*, 1047. (c) Hatcher, L. Q.; Karlin, K. D. *J. Biol. Inorg. Chem.* **2004**, *9*, 669. (d) Schindler, S. *Eur. J. Inorg. Chem.* **2000**, 2311.

- (4) (a) Karlin, K. D.; Nasir, M. S.; Cohen, B. I.; Cruse, R. W.; Kaderli, S.; Zuberbühler, A. D. *J. Am. Chem. Soc.* **1994**, *116*, 1324. (b) Pidcock, E.; Obias, H. V.; Zhang, C. X.; Karlin, K. D.; Solomon, E. I. *J. Am. Chem. Soc.* **1998**, *120*, 7841.
- (5) Santagostini, L.; Gullotti, M.; Monzani, E.; Casella, L.; Dillinger, R.; Tuczek, F. *Chem. Eur. J.* **2000**, *6*, 519.
- (6) Costas, M.; Xifra, R.; Llobet, A.; Solà, M.; Robles, J.; Parella, T.; Stoeckli-Evans, H.; Neuburger, M. *Inorg. Chem.* **2003**, *42*, 4456.
- (7) Liang, H.-C.; Zhang, C. X.; Henson, M. J.; Sommer, R. D.; Hatwell, K. R.; Kaderli, S.; Zuberbühler, A. D.; Rheingold, A. L.; Solomon, E. I.; Karlin, K. D. *J. Am. Chem. Soc.* **2002**, *124*, 4170.

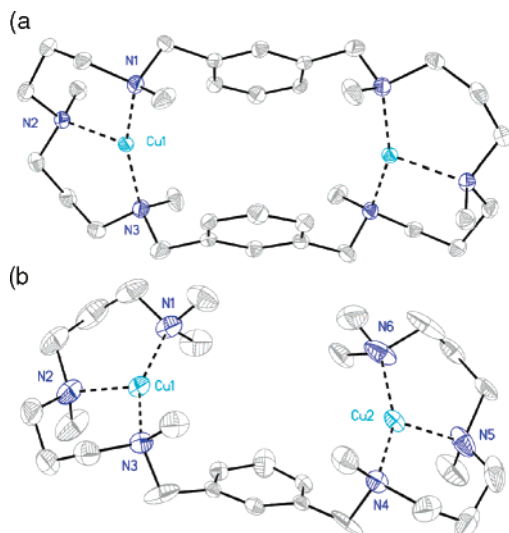


Figure 1. ORTEP diagrams for the cationic part of (a) **1(BArF)₂**: Cu–N1 2.007(3) Å, Cu–N2 2.192(2) Å, Cu–N3 1.999(3) Å, N3–Cu–N1 156.52(10)°, N3–Cu–N2 102.50(10)°, N1–Cu–N2 100.98(10)° and (b) **2(SbF₆)₂**: Cu1–N1 1.990(3) Å, Cu1–N2 2.120(3) Å, Cu1–N3 1.986(3) Å, Cu2–N4 1.974(2) Å, Cu2–N5 2.100(3) Å, Cu2–N6 1.973(3) Å, N3–Cu1–N1 148.84(11)°, N3–Cu1–N2 105.08(10)°, N1–Cu1–N2 105.59(11)°, N6–Cu2–N4 150.62(13)°, N6–Cu1–N5 104.34(15)°, N4–Cu1–N5 104.95(12)°.

L1 and L2 were prepared following a three-step synthetic method involving dialdehyde–amine condensation, NaBH₄ hydrogenation, and HCHO/HCOOH permethylation (see Supporting Information). Dicopper complexes [Cu₂(L1)](X)₂ (**1X₂**) and [Cu₂(L2)](X)₂ (**2X₂**) (X = CF₃SO₃, SbF₆ and BArF; BArF = [B{3,5-(CF₃)₂-C₆H₃]₄][−]) were prepared. **1(BArF)₂** and **2(SbF₆)₂** were characterized by X-ray diffraction analysis.⁸

1(BArF)₂ and **2(SbF₆)₂** contain discrete dinuclear cationic complexes (Figure 1). The coordination geometries and metrical parameters of the metal sites are not very different. Within each complex, the two Cu sites are pseudo or symmetrically related and the Cu···Cu distances are 7.040(3) and 7.019(2) Å, respectively. Each Cu ion contains an N3 coordination set and adopts a distorted trigonal planar geometry. The average Cu–N distance is 2.066(3) Å for **1(BArF)₂** and 2.024(3) Å for **2(SbF₆)₂**. The main difference between the two structures can be found in the N1–Cu1–N3 angle, which is 156.52(10)° in **1(BArF)₂** and 148.84(11)° (150.62–(13)° for the pseudo-symmetrically related N4–Cu2–N6 angle) in **2(SbF₆)₂**, which presumably reflects subtle ligand strains imposed by the more rigid macrocyclic L1 backbone. These structural parameters closely resemble the ones found in [Cu(MeAN)]B(C₆F₅)₄,⁷ where Cu(I) adopts a tricoordinated geometry using a similar nitrogen-based donor-set ligand. The low coordination number and geometry attained in these

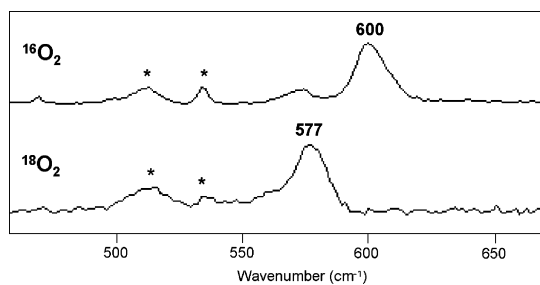


Figure 2. Resonance Raman spectra ($\lambda_{\text{ex}} = 413 \text{ nm}$) of **3** generated from ¹⁶O₂ (top) and from ¹⁸O₂ (bottom) in frozen acetone (77 K). Solvent peaks are marked with an *.

complexes is particularly interesting because it provides available coordination sites for interaction with external molecules such as O₂ and indeed is the most common coordination structure found in Cu-dependent O₂-processing proteins.¹²

Multinuclear NMR studies performed in acetone-*d*₆ for **1(BArF)₂** and **2(BArF)₂** indicated that the solid-state structures are retained in solution. Pulse field gradient spin–echo NMR (PGSE) measurements in acetone-*d*₆ at −80 °C provide diffusion rates of $0.98 \pm 0.12 \times 10^{-11}$ and $0.89 \pm 0.11 \times 10^{-10} \text{ m}^2 \cdot \text{s}^{-1}$ for **1** and **2**, respectively, which indicates that both species have similar hydrodynamic radii, which, in turn, points toward a monomeric nature of the species in solution.^{9,10}

The electronic properties of the metal sites were studied by FT-IR analyses of the corresponding Cu(I)–CO adducts, which were generated in situ by bubbling CO through CH₂-Cl₂ solutions.¹¹ Remarkably, $\nu(\text{CO})$ frequencies are 2083 and 2085 cm^{−1} in **1** and **2**, respectively, which indicates that Cu(I) sites in both complexes are electronically comparable.¹² We conclude that the Cu(I) ions in **1** and **2** possess electronically and structurally analogous properties.

Despite the structural similarities between the complexes described, they show an unexpectedly different reactivity toward O₂. Compound **1X₂** (X = CF₃SO₃ and BArF) does not react with O₂ in acetone at 193 K but irreversibly reacts with O₂ at 273 K to generate copper(II) species. However, no accumulation of any apparent intermediate was detected, and therefore, we conclude that decomposition of any reaction intermediate is always faster than its formation. On the other hand, reaction of **2X₂** (X = CF₃SO₃, SbF₆, and BArF) with O₂ in acetone, CH₂Cl₂, or THF at low temperature shows the relatively fast formation (within seconds) of a yellow species which was formulated as a bis- μ -oxo dicopper(III) species (**3**) on the basis of its UV–vis and resonance Raman spectra. The UV–vis spectrum of **3** in THF at −80 °C exhibits two prominent bands at 308 ($\epsilon = 20\,000 \text{ M}^{-1} \cdot \text{cm}^{-1}$) and 413 nm ($\epsilon = 28\,000 \text{ M}^{-1} \cdot \text{cm}^{-1}$). Resonance Raman experiments carried out in acetone using laser excitation at 413 nm reveal a characteristic Cu₂O₂ breathing vibration peak at 600 cm^{−1} that shows a −23 cm^{−1} downshift when ¹⁸O₂ is used (Figure 2). These are common spectral features for a Cu₂^{III}(μ -O)₂ core which led us to formulate **3** as [Cu₂^{III}(μ -O)₂L₂]²⁺.¹³

(9) (a) Price, W. S. *Concepts Magn. Reson.* **1997**, *9*, 299. (b) Price, W. S. *Concepts Magn. Reson.* **1998**, *10*, 197.

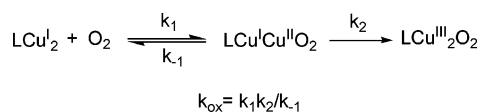
(10) **L1** and **L2** present a similar value of $2.51 \pm 0.17 \times 10^{-10} \text{ m}^2 \cdot \text{s}^{-1}$.

(11) These complexes lose CO when isolated in the solid state.

(12) Attempts to obtain a Cu(II)/Cu(I) redox potential by cyclic voltammetry were unsuccessful.

(8) X-ray crystal data for complex **1(BArF)₂**: C₉₈H₈₂B₂Cu₂F₄₈N₆, $M_f = 2404.40$, monoclinic, space group *P21/n*, $a = 13.073(5) \text{ \AA}$, $b = 27.978(12) \text{ \AA}$, $c = 13.464(6) \text{ \AA}$, $\beta = 96.633(7)^\circ$, $V = 4891(3) \text{ \AA}^3$, $Z = 2$, $T = 100(2) \text{ K}$, $\delta_{\text{calcd}} = 1.633 \text{ Mg} \cdot \text{m}^{-3}$, $\mu = 0.578 \text{ mm}^{-1}$, $R_{\text{int}} = 0.0488$ for 11 668 independent reflections of the 69 618 collected, final indices $I > 2\sigma(I)$; $R1 = 0.0510$, $wR2 = 0.1057$. **2(SbF₆)₂**: C₂₈H₅₆Cu₂F₁₂N₆Sb₂, $M_f = 1075.37$, monoclinic, space group *P21/c*, $a = 16.264(4) \text{ \AA}$, $b = 15.169(4) \text{ \AA}$, $c = 17.642(5) \text{ \AA}$, $\beta = 103.776(4)^\circ$, $V = 4227(2) \text{ \AA}^3$, $Z = 4$, $T = 100(2) \text{ K}$, $\delta_{\text{calcd}} = 1.690 \text{ g} \cdot \text{cm}^{-3}$, $\mu = 2.337 \text{ mm}^{-1}$, $R_{\text{int}} = 0.0351$ for 10 415 independent reflections of the 62 969 collected, final indices $I > 2\sigma(I)$; $R1 = 0.0305$, $wR2 = 0.0772$.

Scheme 2



The diffusion rate for **3** measured in acetone-*d*₆ at -80 °C is $1.25 \pm 0.14 \times 10^{-10} \text{ m}^2 \cdot \text{s}^{-1}$, which compares well with the values obtained for **1** and **2** and strongly supports the intramolecular nature of O₂ binding. **3** constitutes then the first example of a Cu₂^{III}(μ-O)₂ species formed within a dicopper complex containing a xylyl spacer,¹⁴ as to date only intramolecular Cu₂^{II}(μ-η²:η²-O₂) intermediates have been characterized for systems using this type of linker.^{4,5} Besides, despite several examples of [Cu₂^{III}(μ-O)₂L₂] species, where L is a bidentate diamine, have already been reported,³ **3** constitutes a rare example of such species supported by tridentate ligands.^{7,15,16} Although it is well established that Cu₂^{III}(μ-O)₂ species are usually close in energy to their Cu₂^{II}(μ-η²:η²-O₂) isomers,^{3,15} the structure of **3** was found to be unperturbed by either the counterion (CF₃SO₃ or BArF) or the solvent (THF, acetone, or CH₂Cl₂). DFT calculations at the B3LYP level (see Supporting Information) indicate that, for **3**, the Cu₂^{III}(μ-O)₂ structure is 35.5 kJ·mol⁻¹ more stable than Cu₂^{II}(μ-η²:η²-O₂), thus substantiating the sole observation of the bis-μ-oxo isomer. These results clearly contrast those reported by Karlin et al. in the oxygenation of a related mononuclear [Cu(MeAN)]B(C₆F₅)₄,⁷ where side-on Cu₂^{II}(μ-η²:η²-O₂) species are formed.

Stopped-flow kinetic analysis of the oxygenation reactions indicates that **2** reacts reversibly with O₂ to generate **3**.¹⁷ At low temperatures (from -80 to -50 °C), the equilibrium is shifted to the right and the formation of **3** is essentially quantitative. Under these conditions, the reaction is first order in [O₂] and first order in [**2**] (See Supporting Information):

$$v = k_{\text{ox}}[\mathbf{2}][\text{O}_2]$$

Activation parameters for the oxygenation reactions are characterized by a rather low $\Delta H^\ddagger = 9.5 \pm 2 \text{ kJ} \cdot \text{mol}^{-1}$ and a large negative $\Delta S^\ddagger = -175 \pm 10 \text{ J} \cdot \text{K}^{-1} \cdot \text{mol}^{-1}$. The simple second-order rate law observed at low temperature is consistent with a stepwise reaction scheme (Scheme 2) similar to the oxygenation mechanisms of other dicopper(I) complexes.^{3b,17}

This mechanistic picture (Scheme 2) involves reversible reaction of O₂ with **2** to generate a putative superoxo

Cu^ICu^{II}O₂⁻ species in a left-lying pre-equilibrium process, followed by intramolecular collapse into the final dinuclear [Cu₂^{III}(μ-O)₂L₂]²⁺ structure. The kinetic parameters and rate law associated with the formation of **3** resemble those determined for (μ-η²:η²-peroxo)dicopper(II) species bearing tridentate bis(pyridylethyl)amine ligands tethered by *m*-xylyl scaffolds.⁴ It is also interesting to point out that the oxygenation of the related mononuclear [Cu(MeAN)]⁺ complex exhibits a second-order rate law in copper complex.⁷ Comparison between the kinetic parameters associated to the formation of **3** and [Cu₂^{II}(μ-η²:η²-O₂)(MeAN)₂]⁺ indicates a higher ΔH^\ddagger and a lower ΔS^\ddagger for the former, probably associated with its more organized dinuclear structure.¹⁸ Direct interpretation of these parameters is hampered by the different rate law and the multistep nature of the oxygenation reaction. Also unexpected is the dramatic difference in the O₂ reactivity of **1** and **2**. Given the comparable coordination sphere and electronic properties of the Cu(I) ions in both complexes, it is rather unlikely that the initial O₂ binding to a single Cu(I) ($k_1 \cdot k_{-1}^{-1}$) depends on the particular complex, and therefore, the different O₂ reactivity highlights the important role played by the second metal ion. The reaction in complex **1** is slower than in **2**, presumably because there is an enthalpic barrier to surmount to bring the two Cu ions together due to some strain from the ligand. In complex **2**, the ligand is flexible, allowing copper sites to approach close enough to promote their synergistic actuation in O₂ binding/reduction. Instead, the rather rigid nature of the macrocyclic ligand L1 imposes a higher barrier to this process, shutting down the reaction. The stability of **3**, which allows its spectroscopic characterization, in comparison with the lack of stability of any reaction intermediate formed along the **1** + O₂ pathway may also be explained on the basis of the different structural strains imposed by the ligands.

In summary, comparison of the O₂ chemistry associated to [Cu(MeAN)]⁺, **1**, and **2** constitutes a remarkable example of the importance of the cooperative actuation of two metal centers in the activation of O₂ and highlights the challenge in designing suitable dinuclear scaffolds for modeling O₂-processing proteins containing a dimetallic active site.¹⁹

Acknowledgment. Financial support from MEC of Spain through Projects No. CTQ2005-08797-C02-01 and BQU2003-02884, from NIH (GM-38767 to L.Q.), and from NSF (CHE 0111202 to E.R.A.). A.C. is grateful to MEC for the allocation of a Ph.D. grant.

Supporting Information Available: Full details for the preparation and characterization of **1X**₂ and **2X**₂, kinetic data, and details on the computational calculations. CIF files and details of the crystallographic characterization of **1X**₂ and **2X**₂. This material is available free of charge via the Internet at <http://pubs.acs.org>.

IC0602446

- (13) (a) Holland, P.; Cramer, C. J.; Wilkinson, E. C.; Mahapatra, S.; Rodgers, K. R.; Itoh, S.; Taki, M.; Fukuzumi, S.; Que, L., Jr.; Tolman, W. B. *J. Am. Chem. Soc.* **2000**, *122*, 792. (b) Que, L., Jr.; Tolman, W. B. *Angew. Chem., Int. Ed.* **2002**, *41*, 1114.
- (14) Cu₂^{III}(μ-O)₂ species have been described for xylyl-bridged TACN systems, but resulting from intermolecular interaction of Cu ions. See Mahapatra, S.; Kaderli, S.; Llobet, A.; Neuhold, Y.-M.; Palanche, T.; Halfen, J. A.; Young, V., Jr.; Kaden, T. A.; Que, L., Jr.; Zuberbühler, A.; Tolman, W. B. *Inorg. Chem.* **1997**, *36*, 6343.
- (15) Halfen, J. A.; Mahapatra, S.; Wilkinson, E.; Kaderli, S.; Young, V., Jr.; Que, L., Jr.; Zuberbühler, A. D.; Tolman, W. B. *Science* **1996**, *271*, 1397.
- (16) Arii, H.; Saito, Y.; Nagatomo, S.; Kitagawa, T.; Funahashi, Y.; Jitsukawa, K.; Masuda, H. *Chem. Lett.* **2003**, *32*, 156.
- (17) From a kinetic point of view, O₂ binding appears to be essentially irreversible at low temperatures and O₂ release appears to be significant only at higher temperatures. However, analysis of these reactions is complicated by the onset of rapid thermal decomposition.

(18) See ref 7. Reported kinetic parameters for the oxygenation of [Cu(MeAN)]⁺ in CH₂Cl₂ are $\Delta H^\ddagger = -27 \text{ kJ} \cdot \text{mol}^{-1}$ and $\Delta S^\ddagger = -335 \text{ J} \cdot \text{K}^{-1} \cdot \text{mol}^{-1}$.

(19) (a) Bol, J. E.; Driessen, W. L.; Ho, R. Y. N.; Maase, B.; Que, L., Jr.; Reedijk, J. *Angew. Chem., Int. Ed. Engl.* **1997**, *36*, 998. (b) Karlin, K. D.; Dong-Heon, L.; Kaderli, S.; Zuberbühler, A. D. *Chem. Commun.* **1997**, *5*, 475. (c) Tachi, Y.; Aita, K.; Teramae, S.; Tani, F.; Naruta, Y.; Fukuzumi, S.; Itoh, S. *Inorg. Chem.* **2004**, *43*, 4558.